



Projections for Variants of Concern under Austin's COVID-19 Staged- Alert System

Nazlıcan Arslan, David P. Morton, Desmar Walkes, and Lauren Ancel Meyers

October 20, 2021

The University of Texas at Austin
COVID-19 Modeling Consortium

utpandemics@austin.utexas.edu

Projections for Variants of Concern under Austin’s COVID-19 Staged-Alert System

Nazlıcan Arslan¹, David P. Morton¹, Desmar Walkes², and Lauren Ancel Meyers³

¹Industrial Engineering and Management Sciences, Northwestern University

²Austin Public Health

³Integrative Biology, The University of Texas at Austin

October 19, 2021

Overview

To support public health decision-making in Austin, Texas, we use a data-driven model of COVID-19 transmission in the five-county Austin–Round Rock Metropolitan Statistical Area to project hospital demand under plausible scenarios for future COVID-19 transmission. This model integrates Austin’s COVID-19 staged-alert system, which informs the city’s adaptive risk-based guidelines. Given the emergence of SARS-CoV-2 variants and the ongoing roll-out of vaccines, we apply the model to evaluate the robustness of the thresholds governing changes between alert stages.

The projections consider several scenarios for the future transmission of the Delta variant and the emergence of other variants of concern. We assume that Delta is 1.65 times more transmissible than previous variants, has a higher hospitalization rate among symptomatic individuals, has a shorter incubation period, and leads to longer ICU stays. The hypothesized variants of concern are identical to Delta, except that they are instead 2.0 and 2.5 times more transmissible than pre-Delta variants. The results presented here are based on multiple assumptions about the transmission rate, age-specific severity of COVID-19, efficacy of vaccines, waning immunity following infection or vaccination, and uptake of initial two-dose vaccination as well as boosters. They do not represent the full range of uncertainty that the City of Austin may encounter.

The projections suggest that the current threshold for transitioning from Stage 2 (blue) to Stage 1 (green) may fail to guard against future variants of concern. Reducing the threshold from a rolling-average of five new COVID-19 admissions to zero would be expected to reduce risks of rapid resurgences. We are posting these results prior to peer review to provide intuition for both policy makers and the public regarding the near-term threat of COVID-19.

Projections under Delta

The City of Austin uses a five-stage color-coded COVID-19 alert system. Each stage corresponds to a specific combination of social distancing measures and business restrictions [1]. Changes in the alert stage are triggered based on the rolling seven-day average of COVID-19 hospital admissions across all area healthcare systems.

Austin experienced a third wave of the COVID-19 pandemic following the emergence of the highly transmissible Delta variant. Given the unique characteristics of the Delta variant, the ongoing vaccine and booster roll-out, and our evolving understanding of vaccine-acquired and infection-acquired immunity, we made a series of projections to test and, if necessary, update the existing alert system thresholds, which trigger changes in the alert stage.

Figure 1 projects COVID-19 hospital admissions and ICU census under Austin’s staged-alert system, using two different sets of thresholds. The top pair of graphs use the current thresholds, i.e., a 7-day moving average of 5, 15, 30, and 50 daily COVID-19 admissions to trigger changes in green-blue, blue-yellow, yellow-orange, and orange-red alert stages, respectively. The bottom pair of graphs assume identical thresholds, except the transition from blue to green is reduced from five to zero. Under the current thresholds, 3.67% of projections reach the threshold for moving from blue to green. In all of those projections, the shift from blue to green is followed by a rapid spike that could threaten ICU capacity. Under the alternative set of thresholds, such spikes do not occur.

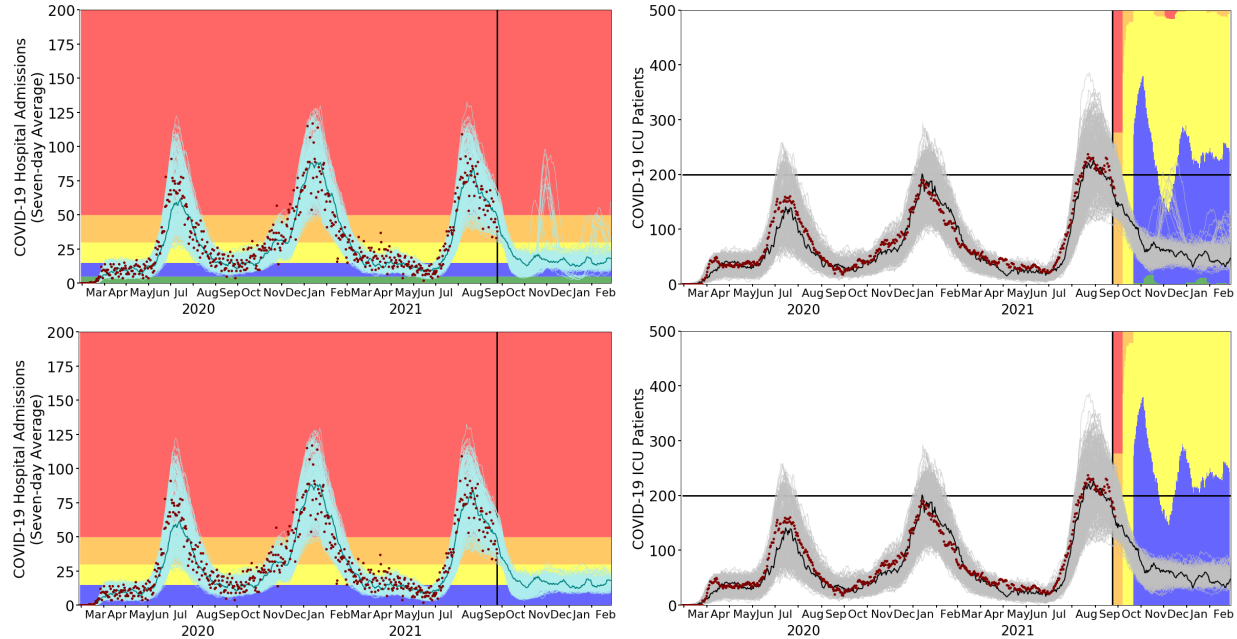


Figure 1: Projected COVID-19 hospital admissions (left) and COVID-19 ICU patient census (right) in the Austin-Round Rock MSA through February 28, 2022, assuming that the Delta variant continues to spread. **Top row:** The projections assume the current thresholds in Austin’s staged-alert system, i.e., a 7-day moving average of 5, 15, 30, and 50 daily COVID-19 admissions trigger changes in the green-blue, blue-yellow, yellow-orange, and orange-red stages, respectively. The red points represent historical data, the black horizontal line represents ICU capacity (200 beds), the light curves indicate stochastic simulations (300 per graph), and solid lines illustrate a representative projection. Note the projected spikes in admissions and ICU census in November and December. These occur shortly after transitions from blue (stage 2) to green (stage 1). The colors in the right-hand plot show the proportion of sample paths that are in each stage at each point in time, including those in green (stage 1) during November. **Bottom row:** The plots are identical to those in the top row except that the threshold for moving from blue to green is reduced from five to zero. None of the 300 projections under this policy resulted in November-December spikes.

Projections under Hypothesized Variants of Concern

To test the robustness of the alert system to future threats, we simulate the emergence of novel variants of concern that are more transmissible than the Delta variant. We estimate that Delta is 1.65 times more transmissible than pre-Delta variants, and causes 80% more hospitalizations among symptomatic individuals. Figures 2 and 3 repeat the analysis of the previous section for hypothesized variants that have the same hospitalization rate as Delta but are 2.0 and 2.5 times more transmissible than pre-Delta variants, respectively. The projections suggest that the current thresholds may leave Austin vulnerable to rapid resurgences in hospitalizations following transitions from blue to green. As with the Delta variant projections above, reducing the blue to green threshold from five to zero COVID-19 admissions would be expected to prevent such surges.

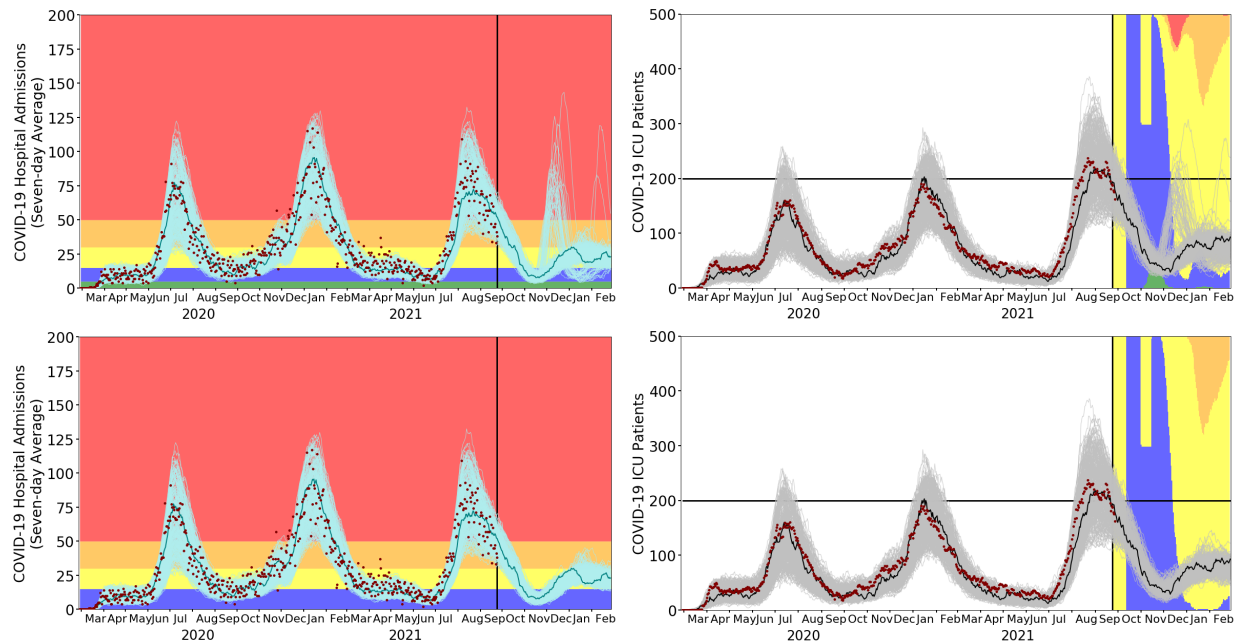


Figure 2: **Projected COVID-19 hospital admissions (left) and COVID-19 ICU patient census (right) in the Austin-Round Rock MSA through February 28, 2022, with a hypothesized variant that is twice as transmissible as pre-Delta variants (roughly 20% more transmissible than Delta)** *Top row:* The projections assume the current thresholds in Austin’s staged-alert system, i.e., a 7-day moving average of 5, 15, 30, and 50 daily COVID-19 admissions trigger changes in the green-blue, blue-yellow, yellow-orange, and orange-red stages, respectively. The red points represent historical data, the black horizontal line represents ICU capacity (200 beds), the light curves indicate stochastic simulations (300 per graph), and solid lines illustrate a representative projection. Note the projected spikes in admissions and ICU census in November and December. These occur shortly after transitions from blue (stage 2) to green (stage 1). The colors in the right-hand plot show the proportion of sample paths that are in each stage at each point in time, including those in green (stage 1) during November. *Bottom row:* The plots are identical to those in the top row except that the threshold for moving from blue to green is reduced from five to zero. None of the 300 projections under this policy resulted in November-December spikes.

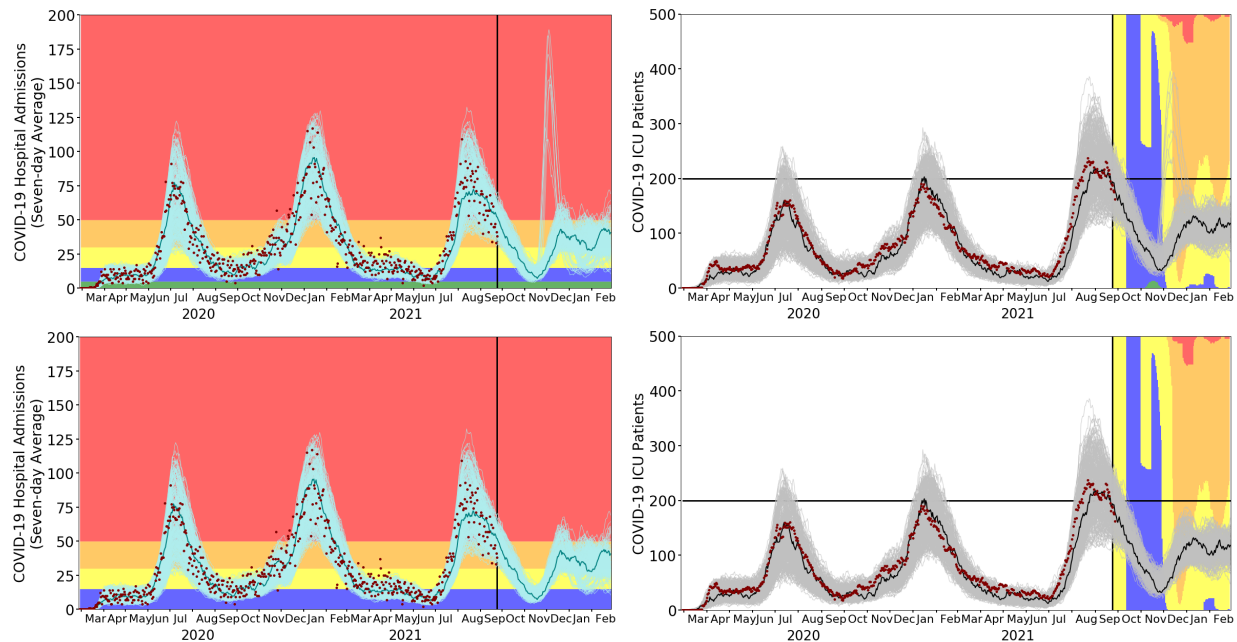


Figure 3: Projected COVID-19 hospital admissions (left) and COVID-19 ICU patient census (right) in the Austin-Round Rock MSA through February 28, 2022, with a hypothesized variant that is 2.5 times as transmissible as pre-Delta variants (roughly 50% more transmissible than Delta) **Top row:** The projections assume the current thresholds in Austin’s staged-alert system, i.e., a 7-day moving average of 5, 15, 30, and 50 daily COVID-19 admissions trigger changes in the green-blue, blue-yellow, yellow-orange, and orange-red stages, respectively. The red points represent historical data, the black horizontal line represents ICU capacity (200 beds), the light curves indicate stochastic simulations (300 per graph), and solid lines illustrate a representative projection. Note the projected spikes in admissions and ICU census in November and December. These occur shortly after transitions from blue (stage 2) to green (stage 1). The colors in the right-hand plot show the proportion of sample paths that are in each stage at each point in time, including those in green (stage 1) during November. **Bottom row:** The plots are identical to those in the top row except that the threshold for moving from blue to green is reduced from five to zero. None of the 300 projections under this policy resulted in November-December spikes.

Appendix

Appendix A describes how we used Texas Department of State Health Services (DSHS) data on the vaccine roll-out to estimate how many people in each age-risk group are vaccinated in our analysis. Appendix B details the update in our model due to the emergence of the Delta variant. Appendix C describes the enhanced SEIR model we used in our analysis. Appendix D details parameters used in the model along with methods for estimating or selecting those parameters.

A Vaccine Allocation

We assume that vaccinations reduce susceptibility to infection, and reduce the severity of outcomes among those infected. Our SEIR model has four “layers” that include individuals who are: (i) unvaccinated, (ii) partially vaccinated, (iii) fully vaccinated or have received a booster, and (iv) vaccinated with waned efficacy after 250 days. Prior to the Delta variant, we assume reductions in susceptibility of 70% for groups (ii) and (iv) and 90% for group (iii), while assuming 95% reduction in severe outcomes for group (ii), (iii), and (iv). Under the Delta variant, we assume reductions in susceptibility of 62%, 70%, and 40% for groups (ii), (iii), and (iv), and respective reductions in severe outcomes of 85%, 95%, and 80% for the same three groups. We assume that individuals who are high-risk, or who are 65 years and older, and initially received the Pfizer vaccine, receive boosters, mimicking their original vaccination schedule, 250 days after their second shot. Low-risk individuals under 65 yo, and those receiving Moderna or J&J vaccines, are assumed to remain in the waned state after 250 days.

We model daily vaccination efforts starting on January 10, 2021, but we account for earlier vaccinations, effective on January 10th. We use DSHS data to estimate how vaccines were allocated across multiple age-risk groups from January 10 to September 24, 2021. In particular, we use data regarding the *first-dose vaccine administration* from DSHS [2] to estimate the number of vaccinated individuals for each age and risk group, across ten such groups: ages 0-4 years-old, 5-17 yo, 18-49 yo, 50-64 yo, and 65 years and older, each with low risk and high risk for severe COVID-19 outcomes. After September 24, 2021 we assume vaccinations continue at the same rate of September 10–24, 2021 until December 15, 2021 or until an assumed uptake rate is achieved.

We assume that every individual who receives a first dose of the vaccine, receives a second dose 21 days later. We assume 97% of the over-65-years-old population is vaccinated. Among 18-64 yo age groups, the vaccine uptake is 95% for high-risk groups and 80% for low-risk groups. For 12-17 yo age groups, the vaccine uptake is 95% for the high-risk group and 40% for low-risk group. Vaccines are not allocated to those under 12 years old. In the rest of this section we provide further details on how we estimate “who was vaccinated when” based on DSHS data.

The COVID-19 vaccination effort in states across the US used a phased roll-out. In Phase 1a, health-care providers and residents of long-term care facilities (LTCF) received vaccines. To account for these vaccinations in our analysis, we assume that healthcare providers are only in age groups 18-49 yo and 50-64 yo and follow a demographic structure like the rest of Austin. We assume LTCF residents are in age group 65 years and older, and the proportion of LTCF residents with high-risk conditions is the same as Austin’s overall high-risk proportions in that age group.

Under the Phase 1b vaccine allocation policy in Texas, those 65 years and older and those 18-64 years old with high risk were prioritized. From DSHS data we have for each week how many individuals 65 years and older received a first-dose vaccine. We assume pro rata allocation among high and low risk individuals over 65 years old. We take into account low risk 16-64 age groups and later, the 12-15 yo low-risk age group as vaccine eligibility expanded to younger age groups. We assume vaccines are administered pro rata among low and high risk groups after eligibility expanded.

Important dates for vaccinations are listed below:

- January 10, 2021: The initial day of vaccination in the model.

- March 15, 2021: Texas expanded eligibility to 50-64 years of age.
- March 29, 2021: Texas opened up vaccination to all individuals 16 year and older.
- May 12, 2021: Adolescents from 12 to 15 years old became eligible for vaccinations.
- September 24, 2021: The booster doses became available for individuals with Pfizer-Biontech vaccines.

B Assumptions on the Delta Variant

The SARS-CoV-2 Delta variant rapidly became the dominant variant in the USA after its introduction. We use an “S-shaped” logistic curve to capture the growth of Delta among new infections in Austin according to genetic sequencing data for Texas [3]. Figure 4 shows the prevalence of Delta variant in Texas. Delta became the dominant variant by July 20, 2021. We assume that the Delta variant is 65% more transmissible [4], the incubation period is shorter [5], and rate of hospitalization is 80% higher [6] compared to earlier dominant virus variants. We note that our projections are relatively insensitive to the specific assumption regarding a 65% increase in transmissibility because we estimate the time-varying reduction in transmission due to the community’s actions.

We also assume that Delta variant decreased the vaccine efficacy against infection from 90% to 70%. However, we assume that vaccines are still highly efficacious against severe infection.

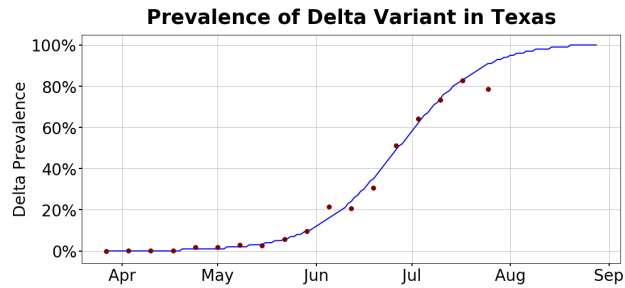


Figure 4: **The Prevalence of Delta Variant in Texas between April and September, 2021.** The red points shows the actual Delta prevalence from genetic sequencing data. The blue line shows the logistic curve fit to the sequencing data. In July 2021, half of the cases were linked to Delta variant.

C Epidemiological Model Overview

Notation:

Indices and Sets

$t \in \mathcal{T}$	set of time periods $\{1, 2, \dots, \mathcal{T} \}$ [day]
$t \in \mathcal{T}_0$	$\mathcal{T} \cup \{0\}$
$a \in \mathcal{A}$	set of age groups $\{0-4y, 5-17y, 18-49y, 50-64y, 65y+\}$
$v \in \mathcal{V}$	set of vaccination status $\{1$ (unvaccinated), 2 (partially vaccinated), 3 (fully vaccinated), 4 (vaccinated but efficacy waned) $\}$
$r \in \mathcal{R}$	risk groups $\{low, high\}$
$i \in \mathcal{I}$	predefined alert stages $\{5$ (red), 4 (orange), 3 (yellow), 2 (blue), 1 (green) $\}$ governing transmission rates
$\omega \in \Omega$	set of simulated spread scenarios

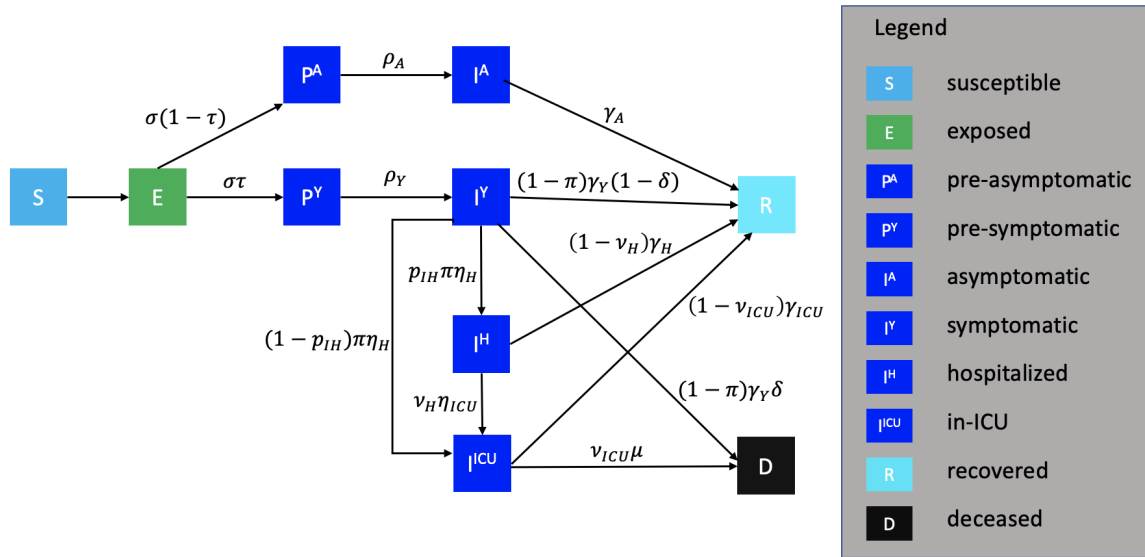


Figure 5: **Compartmental model of COVID-19 transmission in the Austin MSA.** Each subgroup is defined by age and risk as well as vaccine status (unvaccinated, partially vaccinated, fully vaccinated and vaccinated but efficacy waned), and is modeled with a separate set of compartments. Upon infection, susceptible individuals (S) progress to exposed (E) and then to either pre-symptomatic infectious (P^Y) or pre-asymptomatic infectious (P^A) from which they move to symptomatic infectious (I^Y) and asymptomatic infectious (I^A), respectively. All asymptomatic cases eventually progress to a recovered state, where they are assumed to remain protected from future infection (R); symptomatic cases are either hospitalized (I^H), recover or deceased. Mortality (D) varies by age group and risk group.

Parameters

Epidemiological parameters:

β	unmitigated transmission rate
β_v	unmitigated (by NPIs) transmission rate for vaccine status v
σ	rate at which exposed individuals become infectious
τ	proportion of exposed individuals who become symptomatic
τ_v	proportion of exposed individuals who become symptomatic for vaccine status v
ρ_A	rate at which pre-asymptomatic individuals become asymptomatic
ρ_Y	rate at which pre-symptomatic individuals become symptomatic
γ_A	recovery rate from asymptomatic compartment
γ_Y	recovery rate from symptomatic compartment
γ_H^a	recovery rate from hospitalized compartment for age group a
γ_{ICU}^a	recovery rate from ICU compartment for age group a
P	proportion of pre-symptomatic transmission
$YHR^{a,r}$	percent of symptomatic infectious that go to the hospital for age-risk group a, r
η_H	hospitalization rate after symptom onset
ω_A	infectiousness of individuals in IA relative to IY
$\omega_P^{a,r}$	$\frac{P}{1-P} \frac{\tau(YHR^{a,r}/\eta_H + (1-YHR^{a,r})/\gamma_Y) + (1-\tau)\omega_A/\gamma_A}{\tau/\rho_Y + (1-\tau)\omega_A/\rho_A}$: infectiousness of pre-symptomatic individuals relative to IY for age-risk group a, r

$\pi^{a,r}$	$\frac{\gamma_Y \cdot YHR^{a,r}}{[\eta_H - (\eta_H - \gamma_Y)YHR^{a,r}]}$: rate-adjusted proportion of symptomatic individuals who go to the hospital for age-risk group a, r
p_{IH}	percent of patients directly going to the general ward of the hospital
δ	percent of out-of-hospital deaths
$HICUR$	percent of general ward patients who get transferred to ICU
η_{ICU}^a	ICU admission rate after admission to the general ward for age group a
ν_H^a	$\frac{\gamma_H^a \cdot HICUR}{[\eta_{ICU}^a - (\eta_{ICU}^a - \gamma_H^a)HICUR]}$: rate-adjusted proportion of general ward patients transferred to ICU for age group a
μ^a	rate from ICU to death for age group a
$ICUFR^a$	percent of hospitalized that die for age group a
ν_{ICU}^a	$\frac{\gamma_{ICU}^a \cdot ICUFR^a}{[\mu^a - (\mu^a - \gamma_{ICU}^a)ICUFR^a]}$: ICU fatality rate-adjusted proportion for age group a
$\phi_{i,t}^{a',r',a,r}$	expected number of daily contacts from (a', r') to (a, r) at time t under stage i
$N^{a,r}$	population of age-risk group a, r
C_t	vaccine supply at time t

Variables

Epidemiological variables (for scenario $\omega \in \Omega$):

$S_{t,\omega}^{a,r,v}$	number of susceptible people of age group a , risk group r , and vaccine status v at time t [persons]
$dS_{t,\omega}^{a,r,v}$	$S_{t,\omega}^{a,r,v} - S_{t+1,\omega}^{a,r,v}$ [persons]
$E_{t,\omega}^{a,r,v}$	number of exposed people of age group a , risk group r , and vaccine status v at time t [persons]
$PA_{t,\omega}^{a,r,v}$	number of pre-asymptomatic people for a, r, v, t [persons]
$PY_{t,\omega}^{a,r,v}$	number of pre-symptomatic people for a, r, v, t [persons]
$IA_{t,\omega}^{a,r,v}$	number of infectious-asymptomatic people for a, r, v, t [persons]
$IY_{t,\omega}^{a,r,v}$	number of infectious-symptomatic people for a, r, v, t [persons]
$IH_{t,\omega}^{a,r,v}$	number of infected-hospitalized people in the general ward for a, r, v, t [persons]
$ICU_{t,\omega}^{a,r,v}$	number of infected-hospitalized people in the ICU for a, r, v, t [persons]
$R_{t,\omega}^{a,r,v}$	number of recovered people for a, r, v, t [persons]
$D_{t,\omega}^{a,r,v}$	number of deceased people for a, r, v, t [persons]
$H_{t,\omega}$	daily hospital admissions, from infectious-symptomatic to the general ward and ICU, at time t [persons/day]
$\bar{H}_{t,\omega}$	seven-day moving average of $H_{t,\omega}$ [persons/day]
$U_{t,\omega}$	daily ICU admissions (from infectious-symptomatic and the general ward) at time t [persons/day]
$Y_t^{a,r,v',v}$	number of individuals transitioned between compartment due to changing vaccine status from group v' to group v at time t for a, r [persons]

Indicator variables:

$X_{i,t,\omega}$	1 if the system is in alert stage i at time t for scenario ω ; 0 otherwise
------------------	---

We refer to Table 6 for further details on model parameters. We first define the epidemiological transition dynamics in the following equations for all $\omega \in \Omega$. These dynamics largely follow the formulation used in [7] with the addition of three compartments to improve model fidelity and to distinguish beds in the ICU and general ward. The initial conditions specify a single infectious individual in the 18-49 age group with low risk. The age-risk groups are initialized with the rest of the population in their respective susceptible compartments. Eqs. [1a]-[1m] below then provide a sample path, indexed by ω , for the progression of the disease in the community. For the moment, the indicator variables $X_{i,t,\omega} \in \{0, 1\}$ are taken as input, and select the current stage and, in turn, the expected number of daily

contacts via $\phi_{i,t}^{a',r',a,r}$. The contact matrices are indexed by t because they capture whether school is currently open and if so, the school calendar; they further capture weekdays versus weekends and the level of cocooning, which can vary with time; and they capture contacts at school, home, work, and another catch-all category. We assume that sufficient precautions are taken in hospitals so that hospitalized cases do *not* contribute to infecting others via Eq. [1m]. However, we assume an infected vaccinated individual can infect the unvaccinated as much as an infected unvaccinated individual. The most significant updates of the model from that in [7] and [8] are in additional compartments. We use constructs similar to He et al. [9] for a pre-symptomatic period to more accurately model the profile of infectiousness of individuals by including pre-symptom onset transmission. We also model the ICU compartment explicitly for two reasons. First, patients in the ICU have different durations in the hospital than those in the general ward, and second it allows us to account for ICU capacity as a resource. We let p_{IH} denote the probability a hospitalized patient is admitted to a general ward bed and the remaining fraction go directly to the ICU. As Fig. 5 and Eq. [1h] indicate, it is possible to transfer general ward patients to the ICU later if needed. In order to better estimate the recorded deaths for possible vaccination scenarios, we consider in-hospital and out-of-hospital deaths. As Fig. 5 and Eq. [1l] indicate, deaths are recorded either from the ICU (in-hospital) or from the symptomatic individuals that are not hospitalized (out-of-hospital).

For simplicity, we write the finite-difference Eqs. [1] in a deterministic form. They become stochastic, and require indexing by ω , because binomial random variables replace terms like $\sigma E_{t,\omega}^{a,r,v}$; here the binomial random variable has parameter $n = E_{t,\omega}^{a,r,v}$ and σ serves as the ‘‘success’’ probability. This construct is pervasive throughout right-hand side terms in Eqs. [1]. In addition to these ‘‘micro’’ stochastics there are ‘‘macro’’ stochastics because we model σ , ω_A , γ_A , and γ_Y as random variables that are subject to a Monte Carlo draw at time 0 of the simulation.

The following equations hold for all $\forall t \in \mathcal{T}_0$, $a \in \mathcal{A}$, $r \in \mathcal{R}$, $v \in \mathcal{V}$:

$$S_{t+1,\omega}^{a,r,v} - S_{t,\omega}^{a,r,v} = -dS_{t,\omega}^{a,r,v} \quad [1a]$$

$$E_{t+1,\omega}^{a,r,v} - E_{t,\omega}^{a,r,v} = dS_{t,\omega}^{a,r,v} - \sigma E_{t,\omega}^{a,r,v} \quad [1b]$$

$$PA_{t+1,\omega}^{a,r,v} - PA_{t,\omega}^{a,r,v} = \sigma(1 - \tau_v)E_{t,\omega}^{a,r,v} - \rho_A PA_{t,\omega}^{a,r,v} \quad [1c]$$

$$IA_{t+1,\omega}^{a,r,v} - IA_{t,\omega}^{a,r,v} = \rho_A PA_{t,\omega}^{a,r,v} - \gamma_A IA_{t,\omega}^{a,r,v} \quad [1d]$$

$$PY_{t+1,\omega}^{a,r,v} - PY_{t,\omega}^{a,r,v} = \sigma \tau_v E_{t,\omega}^{a,r,v} - \rho_Y PY_{t,\omega}^{a,r,v} \quad [1e]$$

$$IY_{t+1,\omega}^{a,r,v} - IY_{t,\omega}^{a,r,v} = \rho_Y PY_{t,\omega}^{a,r,v} - (1 - \pi^{a,r})\gamma_Y IY_{t,\omega}^{a,r,v} - \pi^{a,r}\eta_H IY_{t,\omega}^{a,r,v} \quad [1f]$$

$$IH_{t+1,\omega}^{a,r,v} - IH_{t,\omega}^{a,r,v} = p_{IH}\pi^{a,r}\eta_H IY_{t,\omega}^{a,r,v} - (1 - \nu_H^a)\gamma_H^a IH_{t,\omega}^{a,r,v} - \nu_H^a \eta_{ICU}^a IH_{t,\omega}^{a,r,v} \quad [1g]$$

$$ICU_{t+1,\omega}^{a,r,v} - ICU_{t,\omega}^{a,r,v} = (1 - p_{IH})\pi^{a,r}\eta_H IY_{t,\omega}^{a,r,v} + \nu_H^a \eta_{ICU}^a IH_{t,\omega}^{a,r,v} - \quad [1h]$$

$$(1 - \nu_{ICU}^a)\gamma_{ICU}^a ICU_{t,\omega}^{a,r,v} - \nu_{ICU}^a \mu^a ICU_{t,\omega}^{a,r,v} \quad [1i]$$

$$R_{t+1,\omega}^{a,r,v} - R_{t,\omega}^{a,r,v} = \gamma_A IA_{t,\omega}^{a,r,v} + (1 - \pi^{a,r})\gamma_Y \delta IY_{t,\omega}^{a,r,v} + (1 - \nu_H^a)\gamma_H^a IH_{t,\omega}^{a,r,v} + \quad [1j]$$

$$(1 - \nu_{ICU}^a)\gamma_{ICU}^a ICU_{t,\omega}^{a,r,v} \quad [1k]$$

$$D_{t+1,\omega}^{a,r,v} - D_{t,\omega}^{a,r,v} = \nu_{ICU}^a \mu^a ICU_{t,\omega}^{a,r,v} + (1 - \pi^{a,r})\gamma_Y (1 - \delta) IY_{t,\omega}^{a,r,v} \quad [1l]$$

$$dS_{t,\omega}^{a,r,v} = S_{t,\omega}^{a,r,v} \sum_{a' \in \mathcal{A}} \sum_{r' \in \mathcal{R}} \sum_{v' \in \mathcal{V}} \sum_{i \in \mathcal{I}} \frac{\beta_v \phi_{i,t}^{a',r',a,r} X_{i,t,\omega}}{N^{a',r'}} \left(IY_t^{a',r',v'} + \omega_A IA_t^{a',r',v'} + \omega_P^{a',r'} \omega_A PA_t^{a',r',v'} + \omega_P^{a',r'} PY_t^{a',r',v'} \right). \quad [1m]$$

The initial conditions have all variables indexed by $t = 0$ as zero except the following:

$$IY_{0,\omega}^{18-49,low} = 1, S_{0,\omega}^{18-49,low} = N^{18-49,low} - 1, \text{ and } S_{0,\omega}^{a,r} = N_{a,r} \forall (a,r) \in \mathcal{A} \times \mathcal{R} \setminus \{(18-49, low)\}. \quad [2]$$

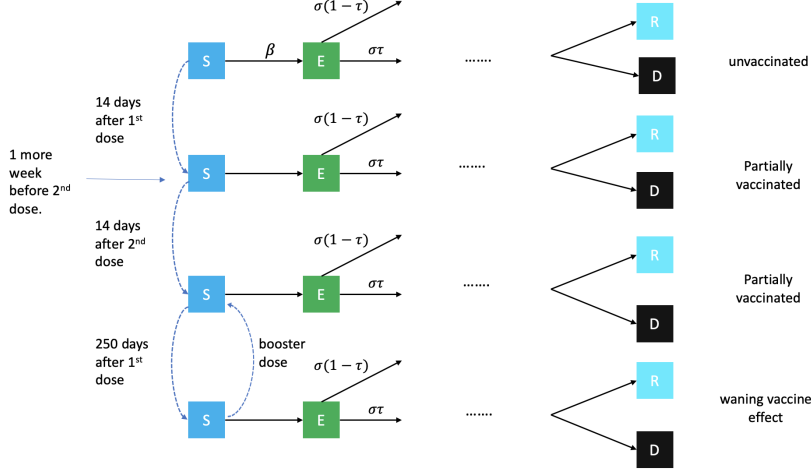


Figure 6: **Compartmental model of COVID-19 transmission in the Austin MSA.** The model from Figure 5 is replicated for each of the four vaccine layers: unvaccinated, partially vaccinated, fully vaccinated and vaccinated but efficacy waned. Individuals transition from one layer to the next based on historical data and based on projections, while accounting for different age-risk categories

We assume vaccine can be administered to susceptible, exposed, infected or recovered individuals but it will have an effect only on susceptible individuals. Vaccines provide protection 14 days after vaccination, second doses are administered 21 days after the first dose and vaccine efficacy wanes 250 days after first dose. Individuals who received a booster shot transition back to fully vaccinated compartment. Eq. [3] captures these vaccination dynamics:

$$S_{t,\omega}^{a,r,v} \leftarrow S_{t,\omega}^{a,r,v} - \sum_{v' \in \mathcal{V}} \frac{S_{t,\omega}^{a,r,v}}{N_{t,\omega}^{a,r,v}} Y_t^{a,r,v,v'} + \sum_{v' \in \mathcal{V}} \frac{S_{t,\omega}^{a,r,v'}}{N_{t,\omega}^{a,r,v'}} Y_t^{a,r,v',v} \quad \forall t \in \mathcal{T}_0, a \in \mathcal{A}, r \in \mathcal{R} \quad [3]$$

D Model Parameters

Table 1 partitions the population of the Austin MSA based on age groups (0-4 years old, 5-17 years old, 18-49 years old, 50-64 years old, and 65 years and older) and risk groups (low risk and high risk). The high-risk group proportions are estimated based on the population with chronic conditions listed by the CDC 500 cities data [10]. Population data processing is detailed in the appendix of [7] and here we present only the final numbers used for this paper’s analysis.

$N^{a,r}$	0-4	5-17	18-49	50-64	65 and older
Low risk	128527	327148	915894	249273	132505
High risk	9350	37451	156209	108196	103763

Table 1: Austin age-risk group populations.

We define four baseline contact matrices, \mathcal{H} , \mathcal{S} , \mathcal{W} , and \mathcal{O} , to describe the contact frequency between age groups at home, at school, at work, and at other locations. These *baseline* matrices assume there is no difference in contacts among the low- and high-risk groups. Each row and column represents an age group, in the order of 0-4 years old, 5-17 years old, 18-49 years old, 50-64 years old, and 65 years old and above, with the row-column value corresponding to a “from-to” transmission contact:

$$\mathcal{H} = \begin{bmatrix} 0.5 & 0.9 & 2.0 & 0.1 & 0.0 \\ 0.2 & 1.7 & 1.9 & 0.2 & 0.0 \\ 0.2 & 0.9 & 1.7 & 0.2 & 0.0 \\ 0.2 & 0.7 & 1.2 & 1.0 & 0.1 \\ 0.1 & 0.7 & 1.0 & 0.3 & 0.6 \end{bmatrix} \quad \mathcal{S} = \begin{bmatrix} 1.0 & 0.5 & 0.4 & 0.1 & 0.0 \\ 0.2 & 3.7 & 0.9 & 0.1 & 0.0 \\ 0.0 & 0.7 & 0.8 & 0.0 & 0.0 \\ 0.1 & 0.8 & 0.5 & 0.1 & 0.0 \\ 0.0 & 0.0 & 0.1 & 0.0 & 0.0 \end{bmatrix}$$

$$\mathcal{W} = \begin{bmatrix} 0.0 & 0.0 & 0.0 & 0.0 & 0.0 \\ 0.0 & 0.1 & 0.4 & 0.0 & 0.0 \\ 0.0 & 0.2 & 4.5 & 0.8 & 0.0 \\ 0.0 & 0.1 & 2.8 & 0.9 & 0.0 \\ 0.0 & 0.0 & 0.1 & 0.0 & 0.0 \end{bmatrix} \quad \mathcal{O} = \begin{bmatrix} 0.7 & 0.7 & 1.8 & 0.6 & 0.3 \\ 0.2 & 2.6 & 2.1 & 0.4 & 0.2 \\ 0.1 & 0.7 & 3.3 & 0.6 & 0.2 \\ 0.1 & 0.3 & 2.2 & 1.1 & 0.4 \\ 0.0 & 0.2 & 1.3 & 0.8 & 0.6 \end{bmatrix}.$$

The contact matrices $\phi_{i,t}^{a',r',a,r}$ are calculated in the same way as Table S6 in [7], considering the effect of weekends, holidays, school closures, and social distancing and cocooning of high-risk populations based on the risk stage. Stages correspond to distancing stages of different strictness, which govern the reduced number of daily contacts people make relative to baseline. In our model, this is reflected by a coefficient $\kappa_i, i \in \mathcal{I}$, where $\kappa_i = 0.75$ would reduce the expected number of contacts to 25% of the baseline value. For the age group of 65 years and older and for the high-risk group, we use reductions based on cocooning, which are represented by coefficients $c_i, i \in \mathcal{I}$:

$$\phi_{i,t}^{a',r',a,r} = \begin{cases} (1 - \kappa_i) [(1 - 1_{\{\text{off day}\}}) \cdot (1 - 1_{\{\text{school closure}\}}) \cdot \mathcal{S}_{a',a} + & \text{if } a', a \in \{0\text{-4yr}, 5\text{-17yr}, 18\text{-49yr}, 50\text{-64yr}\}, \\ (1 - 1_{\{\text{off day}\}}) \cdot \mathcal{W}_{a',a} + \mathcal{H}_{a',a} + \mathcal{O}_{a',a}] & r', r \neq \text{high-risk} \\ (1 - c_i) [(1 - 1_{\{\text{off day}\}}) \cdot (1 - 1_{\{\text{school closure}\}}) \cdot \mathcal{S}_{a',a} + & \\ (1 - 1_{\{\text{off day}\}}) \cdot \mathcal{W}_{a',a} + \mathcal{H}_{a',a} + \mathcal{O}_{a',a}] & \text{otherwise.} \end{cases} \quad [4]$$

The indicator $1_{\{\text{off day}\}}$ takes value 1 if the day is a weekend or holiday and is otherwise 0, and a similar indicator accounts for school closures. When a high-risk group, along with those 65 years and older, is involved either on the “giving” or “receiving” end of a contact, Eq. [4] assumes reduced transmission via the cocooning coefficient, c_i .

The following are key dates during the pandemic in Texas, and some define time blocks, which we use in estimating time-varying transmission reduction factors and other key model parameters as we describe shortly:

- February 28, 2020: Seed date for simulation of Austin, assuming seeding by a single symptomatic individual age 18-49 yo. This corresponds to 14 days prior to the first detected COVID-19 case in Austin on March 13, 2020.
- March 24, 2020: Austin’s Stay Home-Work Safe Order is enacted at midnight [11].
- May 1, 2020: The Governor of Texas relaxed social distancing orders statewide [12].
- May 21, 2020: Just prior to Memorial Day Weekend.
- June 26, 2020: The Governor of Texas issued an executive order limiting service at bars and restaurants, and Travis County (which includes Austin) banned gatherings of more than 100 people [13, 14].
- July 17, 2020: Time point in hospitalization data suggesting a change in dynamics.
- August 20, 2020: First day students returned to residence halls at the University of Texas at Austin.
- October 29, 2020: Apparent COVID-19 fatigue leads to rise in cases

- November 29, 2020: Right after Thanksgiving holiday.
- December 30, 2020: Right before Christmas break end.
- January 10, 2021: The initial day of vaccination in the model.
- March 13, 2021: Austin moved down to alert stage 3.
- May 18, 2021: Austin moved down to alert stage 2.
- July 23, 2021: Delta variant has become the dominant virus type, Austin increased restrictions to stage 4.
- August 5, 2021: Austin increased restrictions to alert stage 5.
- September 24, 2021: The last day of observed data used in estimating model parameters and vaccine allocations.

We assume that there are fourteen time blocks denoted by \mathcal{T}_j for $j \in \{1, \dots, 14\}$ as defined in Table 2. They guide fitting of transmission-reduction parameters, κ and c , and certain dynamics in use of the ICU and hospital duration, as detailed below.

Time Block	Start Date	End Date	Definition
\mathcal{T}_1	2/28/20	3/23/20	unmitigated transmission before first stay-home order
\mathcal{T}_2	3/24/20	5/20/20	effective period for first stay-home order
\mathcal{T}_3	5/21/20	6/25/20	relaxed period starting with Memorial Day weekend
\mathcal{T}_4	6/26/20	7/16/20	period of effective social distancing
\mathcal{T}_5	7/17/20	8/19/20	period distinguished by changes in ICU dynamics
\mathcal{T}_6	8/20/20	10/28/20	period of effective social distancing
\mathcal{T}_7	10/29/20	11/29/20	period of effective social distancing
\mathcal{T}_8	11/30/20	12/30/20	period of effective social distancing
\mathcal{T}_9	12/31/20	01/11/21	period of effective social distancing
\mathcal{T}_{10}	01/12/21	03/12/21	period of effective social distancing and vaccination
\mathcal{T}_{11}	03/13/21	06/19/21	period of effective social distancing and vaccination
\mathcal{T}_{12}	06/20/21	07/30/21	period of less effective social distancing; vaccinations continue
\mathcal{T}_{13}	07/31/21	8/21/21	Delta variant has become dominant variant (past this end date)
\mathcal{T}_{14}	08/22/21	09/24/21	period of effective social distancing and vaccination

Table 2: The time blocks, $\mathcal{T}_1, \mathcal{T}_2, \mathcal{T}_3, \mathcal{T}_4 \cup \mathcal{T}_5, \mathcal{T}_6, \mathcal{T}_7, \mathcal{T}_8, \mathcal{T}_9, \mathcal{T}_{10}, \mathcal{T}_{11}, \mathcal{T}_{12}, \mathcal{T}_{13}$, and \mathcal{T}_{14} correspond to different rates of spread, as estimated using transmission-reduction factors κ and c . The fourth and fifth time blocks, \mathcal{T}_4 and \mathcal{T}_5 , differ only in dynamics involving the ICU, both the admission probability and the sojourn time in the general ward prior to ICU admission.

We model the hospitalization dynamics, including proportions of hospitalized requiring the ICU, durations in the general ward and ICU, and ICU mortality rate using data from a multi-facility hospital system serving the central Texas region, including Austin, Texas (“hospital system data”). While we model differences based on five age groups, we assume the same hospital dynamics in different hospital systems after a patient is admitted across Austin due to similar medical standards. Conditional on being admitted to the hospital, we observe a decreasing trend in the probability a patient is admitted to the ICU throughout the time horizon, which holds for both direct admissions to the ICU and patients who are first admitted to the general ward. Among patients who enter the general ward and are then admitted to the ICU, their duration of stay in the general ward, determined by η_{ICU} , grows over time. For each time block, \mathcal{T}_j , we assume a constant $\eta_{ICU,j}$ and further assume a constant daily decrease, r_j , on both of the fractions, p_{IH} and $HICUR$:

$$p_{IH,t+1} = r_j p_{IH,t} \quad \forall j \in \{1, \dots, 14\}, t \in \mathcal{T}_j \quad [5a]$$

$$HICUR_{t+1} = r_j HICUR_t \quad \forall j \in \{1, \dots, 14\}, t \in \mathcal{T}_j, \quad [5b]$$

along with a similar decrement across boundaries of the blocks. We use duration times for each time block from the hospital system data to estimate $\eta_{ICU,j}^a$ and fit r_j , with the estimated parameters in Table 3.

	age group	\mathcal{T}_1	\mathcal{T}_2	\mathcal{T}_3	\mathcal{T}_4	$\mathcal{T}_5 \cup \dots \cup \mathcal{T}_{14}$
$\eta_{ICU,j}^a$	0-4 yr	0.5882	0.5882	0.3885	0.2640	0.2589
	5-17 yr	0.5882	0.5882	0.3885	0.2640	0.2589
	18-49 yr	0.5882	0.5882	0.3885	0.2640	0.2589
	50-64 yr	0.6273	0.6273	0.4143	0.2815	0.2761
	≥ 65 yr	0.6478	0.6478	0.4278	0.2907	0.2851
r_j		0.9973	0.9973	0.9932	0.9921	1

Table 3: Estimates of ICU admission probability parameters, η_{ICU} , p_{IH} , and $HICUR$; see Fig. 5 and accompanying parameter definitions. For each age group, a , and each time block, j , we specify η_{ICU} , and we give the daily decrement factor, r_j , used in Eq. [5].

Using the hospital system data, and consistent with the transition diagram in Fig. 5, we define the ICU duration for a patient as the time between their admission to the ICU and their discharge from the hospital. The reality is more complex as ICU patients typically return to the general ward prior to discharge from the hospital, and iterations between the two units, driven by a patient's health status, can also occur. Therefore, the reported duration in the ICU leads to over estimating ICU utilization and under-estimating that of the general ward. To handle this in our model, we introduce three constant parameters, α_{ICU} , α_H and α_D , to better estimate durations in the ICU and general ward and ICU mortality rate and better represent their respective utilization:

$$\begin{aligned}\gamma_H &= (1 - \alpha_H)\gamma_H^0 \\ \gamma_{ICU} &= (1 + \alpha_{ICU})\gamma_{ICU}^0 \\ \mu &= (1 + \alpha_D)\mu^0,\end{aligned}$$

where γ_H^0 , γ_{ICU}^0 , and μ^0 are obtained from the hospital system data, with each row corresponding to an age group in ascending order:

$$\gamma_H^0 = \begin{bmatrix} 0.2399 \\ 0.2399 \\ 0.2399 \\ 0.2222 \\ 0.2124 \end{bmatrix}, \quad \gamma_{ICU}^0 = \begin{bmatrix} 0.0700 \\ 0.0700 \\ 0.0700 \\ 0.0575 \\ 0.0518 \end{bmatrix}, \quad \mu^0 = \begin{bmatrix} 0.0749 \\ 0.0749 \\ 0.0749 \\ 0.0766 \\ 0.0799 \end{bmatrix},$$

with units of day^{-1} .

The bulk of the epidemiological and hospitalization parameters are specified above or are detailed in Tables 6 and 7, with the latter obtained from the literature or information collected from local healthcare agencies. The time blocks are specified in Table 2. Given these, we estimate 32 parameters, but with 17 degrees of freedom, as we detail below. We perform the fit of the deterministic SEIR model in Eqs. [1] using: (i) daily COVID-19 admissions, denoted H_t ; (ii) a daily COVID census in the general ward, IH_t ; (iii) a daily COVID census in the ICU, ICU_t ; (iv) daily COVID-19 in-hospital deaths, D_t^H ; and (v) daily COVID-19 out-of-hospital deaths obtained from [15], D_t^{OH} , all on day t . By minimizing a weighted sum of least-square errors, we estimate $\hat{\kappa}_j$ and \hat{c}_j , $j = 1, 2, \dots, 14$, α_H , α_{ICU} , α_D and δ , using SciPy/Python [16] via `scipy.optimize.least_squares`.

We minimize

$$\sum_t (IH_t - \widehat{IH}_t)^2 + w_{ICU}^2 \sum_t (ICU_t - \widehat{ICU}_t)^2 + w_H^2 \sum_t (H_t - \widehat{H}_t)^2 + w_D^2 \sum_t (D_t^H - \widehat{D}_t^H)^2 + w_D^2 \sum_t (D_t^{OH} - \widehat{D}_t^{OH})^2,$$

where \widehat{IH}_t , \widehat{ICU}_t , \widehat{H}_t , \widehat{D}_t^H , and \widehat{D}_t^{OH} denote the estimated IH_t , ICU_t , H_t , D_t^H , and D_t^{OH} obtained through Eqs. [1]; w_{ICU} , w_H , and w_D are scaling constants; and the sum is over $t \in \mathcal{T}_1 \cup \dots \cup \mathcal{T}_{14}$. We assume $w_{ICU} = 1.50$, $w_H = 7.58$, and $w_D = 10w_H$, as those values approximate magnitudes relative to that of the general ward. To obtain a parsimonious model, we use $\hat{c}_1 = 0$, $\hat{c}_2 = \hat{c}_3 = \hat{\kappa}_2$, $\hat{c}_4 = \hat{c}_5 = \hat{\kappa}_4 = \hat{\kappa}_5$, $\hat{c}_6 = \hat{c}_8 = \hat{\kappa}_4$, $\hat{c}_7 = \hat{\kappa}_2$, $\hat{c}_9 = \hat{\kappa}_9$, and $\hat{c}_t = \hat{\kappa}_t$ for $t \in \{10, 11, 12, 13, 14\}$ which reduces the number of estimated parameters from 32 to 17.

We use the trust region reflective algorithm (`trf`) in `scipy.optimize.least_squares`, with lower and upper bounds on each parameter of 0 and 1, respectively. The algorithm obtains locally optimal values of the parameters, the quality of which has been validated by comparing projections with the observed data. All the remaining parameters are set to their default values (see above and Tables 6 and 7). The fitted values for $\hat{\kappa}_j$ and \hat{c}_j and α_H , α_{ICU} and α_D are given in Table 4.

Austin		
j	$\hat{\kappa}_j$	\hat{c}_j
1	0.0523	0.0000
2	0.7878	0.7878
3	0.6420	0.7878
4	0.8270	0.8270
5	0.8270	0.8270
6	0.7783	0.8270
7	0.7530	0.7878
8	0.6743	0.8270
9	0.8015	0.8015
10	0.8111	0.8111
11	0.6849	0.6849
12	0.5545	0.5545
13	0.6490	0.6490
14	0.6779	0.6779
α_H	0.3016	
α_{ICU}	0.0234	
α_D	1.8486	
δ	0.0030	

Table 4: Fitted transmission reduction parameters, $\hat{\kappa}_j$, and cocooning effectiveness parameters, \hat{c}_j , for each time block \mathcal{T}_j , along with estimated hospitalization duration adjustment parameters, α_H , α_{ICU} , and α_D and the percent of out-of-hospital death δ .

Stages	Example measures	Transmission reduction	Cocooning
<i>red</i>	shelter-in-place order: mask mandate, no public activities, gatherings, or travel	largest (83.05%)	83.05%
<i>orange</i>	mask mandate, no indoor dining, no medium or large gatherings	moderate (73.3%)	73.3%
<i>yellow</i>	mask mandate, partial limitations on indoor dining and bars, no large gatherings	modest (63.62%)	63.62%
<i>blue</i>	new normal: avoid large gatherings, masks and physical distancing recommended	low (53.9%)	53.9%
<i>green</i>	no restrictions	no reduction (0%)	0%

Table 5: Structure and impact of five-stage COVID-19 alert system. Colors indicate stages. For each stage, the table provides example measures, which may evolve with future data on the impact of mitigation strategies and roll-out of surveillance testing. The model assumes high risk sub-populations are sheltered to a greater degree, described as cocooning. Transmission reduction estimates and cocooning numbers are derived from COVID-19 hospital admissions data from the Austin, Texas MSA during a period that included a stay-home order, a re-opening phase that led to an early summer surge, followed by reduced transmission with the implementation of face-mask requirements and reinstatement of other distancing measures.

Parameters	Values	Source
β : transmission rate (pre-Delta)	Austin: 0.06901	[7]
β : transmission rate (Delta)	Austin: 0.11387	[4], [7]
P : proportion of pre-symptomatic transmission (%)	44	[9]
ω_A : infectiousness of individuals in compartment IA , relative to IY	$\omega_A \sim \text{Triangular}(0.29, 0.29, 1.4)$	[17]
τ : symptomatic proportion (%)	57	[18]
ω_P : infectiousness of individuals in pre-symptomatic and pre-asymptomatic compartments, relative to symptomatic and asymptomatic compartments	$\omega_P = \frac{P}{1-P} \frac{\tau(\frac{YHR}{\eta H} + \frac{1-YHR}{\gamma_Y}) + (1-\tau)\frac{\omega_A}{\gamma_A}}{\frac{\tau}{\rho_Y} + (1-\tau)\frac{\omega_A}{\rho_A}}$	
σ : exposed rate (pre-Delta)	$\frac{1}{\sigma} \sim \text{Triangular}(1.9, 2.9, 3.9)$	Based on incubation [19] and pre-symptomatic periods
σ : exposed rate (Delta)	$\frac{1}{\sigma} \sim \text{Triangular}(0.4, 1.4, 2.4)$	[5], [19]
γ_A : recovery rate from compartment IA	$\frac{1}{\gamma_A} \sim \text{Triangular}(3, 4, 5)$	[9]
γ_Y : recovery rate from symptomatic compartment IY	$\frac{1}{\gamma_Y} \sim \text{Triangular}(3, 4, 5)$	[9]
ρ_A : rate at which pre-asymptomatic individuals become asymptomatic	Equal to ρ_Y	[9]
ρ_Y : rate at which pre-symptomatic individuals become symptomatic	$\frac{1}{\rho_Y} = 2.3$	[9]
	Low risk High risk	
IFR : infected fatality ratio, age specific (%)	0.000917 0.00917	Age adjusted from [20]
	0.00218 0.0218	
	0.0339 0.339	
	0.252 2.52	
	0.644 6.44	
	Low risk High risk	
YFR : symptomatic fatality ratio, age specific (%)	0.00161 0.0161	$YFR = \frac{IFR}{1-\tau}$
	0.00382 0.0382	
	0.0594 0.594	
	0.442 4.42	
	1.13 11.3	

Table 6: Model parameters

Parameters	Value	Source	
η_H : rate from symptom onset to hospital admission	0.1695	5.9 day average from symptom onset to hospital admission [21]	
YHR : symptomatic case hospitalization rate (%) (pre-Delta)	Low risk	High risk	Age adjusted from [20]
	0.0279	0.2791	
	0.0215	0.2146	
	1.3215	13.2514	
	2.8563	28.5634	
YHR : symptomatic case hospitalization rate (%) (Delta)	Low risk	High risk	[6], [20]
	0.0502	0.5024	
	0.0387	0.3863	
	2.3787	23.8525	
	5.1413	51.4141	
6.0971	60.9714		
p_{IH}	Fitted time series, starting at 0.6717	hospital system data	
γ_H, γ_{ICU} : recovery rate in compartment IH and ICU	Fitted parameters	hospital system data	
π : rate symptomatic individuals go to hospital, age-specific	$\pi = \frac{\gamma_Y \cdot YHR}{\eta_H + (\gamma_Y - \eta_H) YHR}$		
η_{ICU} : rate from hospital admission to ICU	A time series which is constant specific to time blocks	hospital system data	
μ : rate from ICU to death	Fitted parameters	hospital system data	
$ICUFR$: ICU death ratio, age specific (%)	$ICUFR$		hospital system data
	5.8592		
	5.8592		
	5.8592		
	15.6207		
30.8526			
$HICUR$: hospitalized ICU ratio	A time series with a decreasing rate specific to time blocks, starting at 0.1574	hospital system data	
ν_H : ICU rate on hospitalized individuals, age-specific	$\nu_H = \frac{\gamma_H * HICUR}{\eta_{ICU} + (\gamma_H - \eta_{ICU}) HICUR}$		
ν_{ICU} : death rate on ICU individuals, age-specific	$\nu_{ICU} = \frac{\gamma_{ICU} * ICUFR}{\mu + (\gamma_{ICU} - \mu) ICUFR}$		
B : Total hospital bed capacity (including ICU)	Austin: 1500	Estimates provided by each of the region's hospital systems and aggregated by regional public health leaders	
B_{ICU} : ICU capacity	Austin: 331	Estimates provided by each of the region's hospital systems and aggregated by regional public health leaders	
$1_{\{\text{school closure}\}}$: school closure dates	Austin: 3/19/2020 – 9/8/2020, 5/26/2021 – 8/23/2021		

Table 7: Hospitalization parameters

References

- [1] The City of Austin. Key indicators for staging, COVID-19: Risk-based guidelines (2021). URL <https://austin.maps.arcgis.com/apps/dashboards/0ad7fa50ba504e73be9945ec2a7841cb>.
- [2] Texas DSHS. COVID-19 vaccine information (2021). URL <https://www.dshs.texas.gov/coronavirus/immunize/vaccine.aspx>.
- [3] Shu, Y. & McCauley, J. GISAID: Global initiative on sharing all influenza data—from vision to reality. *Euro-surveillance* **22**, 30494 (2017).
- [4] Allen, H., Vusirikala, A., Flanagan, J., Consortium, C.-U. *et al.* Increased household transmission of COVID-19 cases associated with SARS-CoV-2 variant of concern B. 1.617. 2: a national casecontrol study. *Public Health England* (2021).
- [5] Li, B. *et al.* Viral infection and transmission in a large well-traced outbreak caused by the Delta SARS-CoV-2 variant. *medRxiv* (2021).
- [6] Sheikh, A., McMenamin, J., Taylor, B. & Robertson, C. SARS-CoV-2 Delta VOC in scotland: demographics, risk of hospital admission, and vaccine effectiveness. *The Lancet* (2021).
- [7] Duque, D. *et al.* Timing social distancing to avert unmanageable COVID-19 hospital surges. *Proceedings of the National Academy of Sciences* (2020).
- [8] Yang, H. *et al.* Design of COVID-19 staged alert systems to ensure healthcare capacity with minimal closures. *Nature Communications* (2021).
- [9] He, X. *et al.* Temporal dynamics in viral shedding and transmissibility of COVID-19. *Nature Medicine* **26**, 672–675 (2020).
- [10] Centers for Disease Control and Prevention. 500 cities: Local data for better health (2019). URL <https://www.cdc.gov/500cities/definitions/health-outcomes.htm>.
- [11] The Mayor of the City of Austin. STAY HOME – WORK SAFE ORDER NO. 20200413-009, The City of Austin (2020). URL http://www.austintexas.gov/sites/default/files/files/document_96DEBEEC-E581-05E0-8A3D444404948A84.pdf.
- [12] The Governor of Texas. Executive Order GA18: Relating to the expanded reopening of services as part of the safe, strategic plan to open Texas in response to the COVID-19 disaster (2020). URL https://gov.texas.gov/uploads/files/press/EO-GA-18_expanded_reopening_of_services_COVID-19.pdf.
- [13] The Governor of Texas. Executive Order GA28: Relating to the targeted response to the COVID-19 disaster as part of the reopening of Texas (2020). URL https://gov.texas.gov/uploads/files/press/EO-GA-28_targeted_response_to_reopening_COVID-19.pdf.
- [14] The Mayor of the City of Austin. Order 20200626-016: Stay home, mask, and otherwise be safe (2020). URL <https://www.austintexas.gov/sites/default/files/files/Health/Order%20No.%2020200626-016-StayHome-Mask-Otherwise-Be-Safe.pdf>.
- [15] Texas Department of State Health Services. COVID-19 county trends (2021). URL <https://dshs.texas.gov/coronavirus/>.

- [16] Virtanen, P. *et al.* SciPy 1.0: Fundamental Algorithms for Scientific Computing in Python. *Nature Methods* (2020).
- [17] He, D. *et al.* The relative transmissibility of asymptomatic cases among close contacts. *International Journal of Infectious Diseases* **94**, 145–147 (2020).
- [18] Gudbjartsson, D. F. *et al.* Spread of SARS-CoV-2 in the Icelandic population. *New England Journal of Medicine* **382**, 2302–2315 (2020).
- [19] Lauer, S. A. *et al.* The incubation period of coronavirus disease 2019 (COVID-19) from publicly reported confirmed cases: Estimation and application. *Annals of Internal Medicine* (2020).
- [20] Verity, R. *et al.* Estimates of the severity of coronavirus disease 2019: a model-based analysis. *The Lancet Infectious Diseases* **20**, 669–677 (2020).
- [21] Tindale, L. *et al.* Transmission interval estimates suggest pre-symptomatic spread of COVID-19. *Preprint* (2020).